Flow Measurements in Leading-Edge Vortices

P. M. Sforza,* W. Stasi,† J. Pazienza‡ and M. Smorto§
Polytechnic Institute of New York, Farmingdale, N.Y.

An experimental study of the vortex flowfield over slender delta planforms with sharp leading edges is presented. Complete velocity measurements in this three-dimensional flowfield are obtained by means of a Conrad-type probe used in conjunction with a five-degree-of-freedom traversing mechanism, and flow visualization is achieved by an oil fog technique. Effects of angle of attack, camber, sweepback, etc. are described. A new application of such flows, that of wind energy conversion by means of the Vortex Augmentor Concept (patented and patents pending) developed by the first author, is discussed.

I. Introduction

UNDER certain predictable conditions vortices appear in a flowing fluid. They are real manifestations of an idealized whirling flowfield in which the velocity follows circular streamlines with a magnitude inversely proportional to distance from the center of rotation. Vortices are effective as energy storers since they allow, in a sense, an additional degree of freedom, that of rotation, to an originally uniformly translating flow. A natural example of this energy concentrating capability of vortex flows is the tornado. The senior author has developed a concept which utilizes the unusual aerodynamic characteristics of vortices to design improved wind energy conversion systems.

The keystone here is the generation and control of discrete vortices of high power density by appropriate interaction of aerodynamic surfaces with natural winds of relatively low power density. Suitably designed turbines are used to extract energy from this compacted vortex field. This idea is termed the Vortex Augmentor Concept (VAC) and is described in detail by Sforza.[1,2]

Vortex flows best suited to the VAC are those established by flow separation from highly swept sharp leading edges typical of supersonic aircraft planforms. Some examples of such flows are shown in the review of aircraft vortex phenomena by Sforza.[3]

In the laboratory it is possible to accurately model vortex fields over surfaces with highly swept, sharp leading edges as can be seen in Fig. 1. The central region of the vortex over one side of the cambered delta model is made visible by oil smoke in this wind-tunnel test. Of interest is the fact that the laboratory model length scale and the velocity are on the order of 1 m and 1 m/s, respectively; this is much smaller than the case of full-scale aircraft yet the same patterns are reproduced in the small-scale test. This is so because the separation of the oncoming flow from the wing is caused by the *sharp* leading edges and is therefore essentially independent of the Reynolds number. Comprehensive discussions on flows of this type may be found in Thwaites.[4]

An important fact about such flows, then, is that they are independent of scale. Therefore the VAC, which utilizes vortices formed in a scale-independent manner, is not restricted by size considerations. In addition, extensive use of wind-tunnel experimentation is clearly and cleanly applicable to the design process.

In order to exploit the focusing power of leading-edge vortices for the purposes of wind energy conversion it was necessary to have detailed velocity information on such flowfields. This is clear since the turbines are to be placed in the vortex flow in order to extract shaft power therefrom. Characteristics of the vortex field generated by delta-type aerodynamic surfaces are fairly well understood and have received considerable attention.[5] Detailed measurements of the velocity field over these surfaces have received scant attention, however, primarily due to the extreme difficulty and tediousness typical of strongly three-dimensional flowfield diagnostics. In 1967, an exhaustive review by Timm[6] could identify only two such studies; by 1976 no new investigations had appeared. The first such study was by Earnshaw,[7] the results of which were also presented by Hall.[8] These data are confined to a single, low-angle-of-attack (14.9 deg) case for one flat-plate delta wing with aspect ratio $AR = 1$. The second was by Hummel,[9] who explored the stability of leading-edge vortex flows. Due to the nature of his investigation, detailed data are confined to a single, high-angle-of-attack (31 deg) case for one flat-plate delta wing with aspect ratio $AR = 0.78$. Due to this lack of experimental information an extensive program of wind tunnel testing aimed at providing detailed velocity data for various leading-edge vortex flows was initiated and the results form the basis for this report.

II. Experimental Apparatus

Wind-Tunnel Facility

Experimental investigation was performed in the Polytechnic Aerodynamics Laboratories Environmental

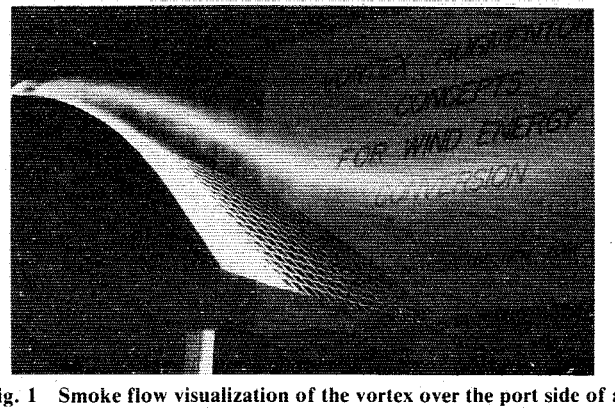

Fig. 1 Smoke flow visualization of the vortex over the port side of a cambered delta.

Received Jan. 7, 1977; presented as Paper 77-11 at the AIAA 15th Aerospace Sciences Meeting, Los Angeles, Calif., Jan. 24-26, 1977; revision received Sept. 2, 1977.

Index categories: Subsonic Flow; Aerodynamics; Wind Power.

*Professor, Aerodynamics Laboratories. Associate Fellow AIAA.

†Research Associate, Aerodynamics Laboratories. Student Member AIAA.

‡Research Assistant, Aerodynamics Laboratories. Presently at Sikorsky Aircraft. Associate Member AIAA.

§Research Assistant, Aerodynamics Laboratories. Student Member AIAA.

Wind Tunnel Test Facility. The wind tunnel is of the open circuit type with a closed test section (1.22 × 1.52 × 6.1 m) and has a normal velocity range between 0.07 and 10.9 m/s.

This study required the use of a special traversing mechanism which was developed at this center. This mechanism provides a probe with five degrees of freedom: three in translation, one in pitch rotation, and one in yaw rotation. The traverse could be incremented in intervals of 0.196 cm accurately, while the pitch and yaw rotation could be incremented in intervals of 1.0 and 1.042 deg, respectively. This movement is obtained by using motorized screw drives for traversing and geared down motors for rotation.

Instrumentation

In order to obtain velocity data in the three-dimensional vortex flowfield a five-hole Conrad-type probe was constructed for use in the traversing mechanism. This probe is capable of determining the direction of the flow by means of two yaw and two pitch pressure taps, and once aligned, its total pressure by means of a central tap. The two pitch pressure taps were connected to a Dwyer Magnehelic differential pressure gage as were the two yaw taps. The yaw lines had the addition of a three-way ball valve in each line, with the second branch from the valves connected to a Y-joint and then to the reference pressure line of an MKS, type 77, Baratron; the total pressure tap of the probe was connected to the high-pressure line of the Baratron. Thus, the local flow direction was determined by balancing the pressure in the yaw and pitch tubes, the difference between the yaw and the total head giving a measurement which could be calibrated for velocity. Calibration of the probe for yaw and pitch nulling and for velocity was accomplished in a smaller wind tunnel with a uniform freestream and is assumed to hold in the vortex flowfields investigated. Nulling the probe with the system just described could be achieved with an accuracy greater than the incrementing capability of the traverse mechanism, and the velocity calibration was repeatable and as consistently accurate as the Dwyer 0.318-cm-diam pitot tube used as a standard.

The outside diameter of the five-hole probe used here is 0.953 cm, which was considered reasonably small in relation to the 40 × 40 cm dimension of the measurement grid used for the vortex flowfield of the wings. A commercially available probe of this type (United Sensors type DC) was originally tried because of its smaller size (0.318 cm diam), but the time response of the probe was found to be too long for the instrumentation system used. A more advanced system utilizing Validyne variable reluctance transducers mounted at the probe itself for measuring all the pressure differentials should improve the time response when the smaller diameter probe is used. This sytem is presently being developed.

The position of the probe on the traversing mechanism was determined by means of digital counters. These counters use a light emitting diode display to show the Y and Z position. The X position, pitch angle, and yaw angle of the probe were obtained by means of mechanical indicators.

The other instruments used in this investigation were a barometer to measure atmospheric pressure, a thermometer to measure freestream temperature, and a Dwyer 0.138-cm-diam pitot probe to measure the freestream velocity. This pitot-static tube was used in conjunction with a Dwyer Magnehelic differential pressure gage.

Test Models

For this investigation six test models of equal span of 61 cm were constructed and tested in the wind tunnel (see Fig. 2). The first test model was a delta wing constructed from 1.27-cm plywood, with 75-deg sweepback, a chamfered leading edge, and an aspect ratio of 1.07. This wing, and the others which follow, were attached to a metal test sting by a single bolt so that they could be easily pivoted to different angles of attack.

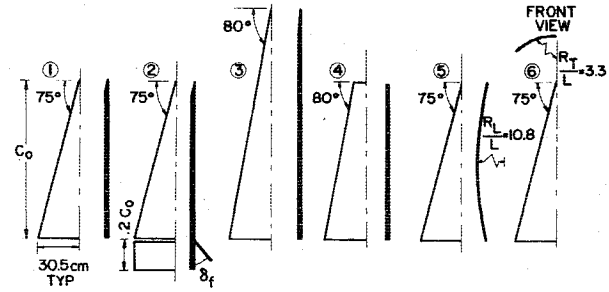

Fig. 2 Schematic diagram of the various test models used in the present study.

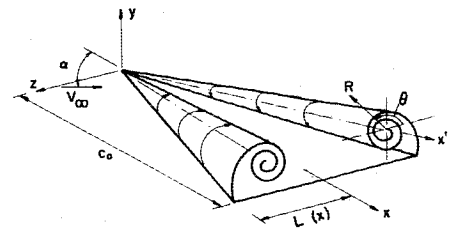

Fig. 3 Coordinate system used in the present study.

The second test model was simply a modification of the previous delta. This modification consisted of a flap, with a chord equal to 20% of the main delta's chord and a span equal to that of the basic delta (aspect ratio = 0.77), made of the same material as the first model. The flap was joined to the main panel by means of a bellcrank such that various flap deflections with respect to the main delta plane could be set.

The third test model was another delta wing but with 80-deg sweepback, chamfered leading edge, and an aspect ratio of 0.71. This model was constructed of 0.32-cm masonite which necessitated securing the wing tips with nylon thread during the tests to prevent flutter.

The fourth test model was constructed from the previous model by the truncation of the top 34% of the delta (this made the model the same length as the first, reference, model); the aspect ratio in this case is 0.71.

The fifth test model was a delta, congruent to the first model but constructed of 0.32-cm masonite so that longitudinal camber could be achieved. This was done by means of a 0.64-cm thick, 3-cm high spine of plywood fashioned such that the upper surface formed a circular arc of radius equal to 330 cm. The ratio of longitudinal radius of curvature to half-span, R_L/L, is therefore 10.8. The delta wing then attached to this spine by means of small angle brackets in order to form the appropriately curved delta surface.

The sixth model was also congruent to the first model but constructed of formica sheet. This sheet was placed in a female form, constructed of plywood, which gave a constant transverse camber in the form of a circular arc of 102 cm radius. The ratio of the transverse radius of curvature to the half-span, R_T/L, is in this case 3.33. The curved sheet was then built up to a thickness of 0.4 cm by means of fiberglass material and epoxy resin. The surface was smoothed, as were all the models, and the leading edge was chamfered.

III. Experimental Results

Data presented here were taken in the plane normal to the main panel at a streamwise station 0.8 C_0 and at a nominal freestream velocity of 7.5 m/s. The coordinate system utilized is illustrated in Fig. 3. Since a great quantity of data was recorded, reduction was accomplished by computer and only a small portion can be readily presented. For the purposes of this report contours of velocity magnitude over half the span at the measurement station are shown, along with vortex core

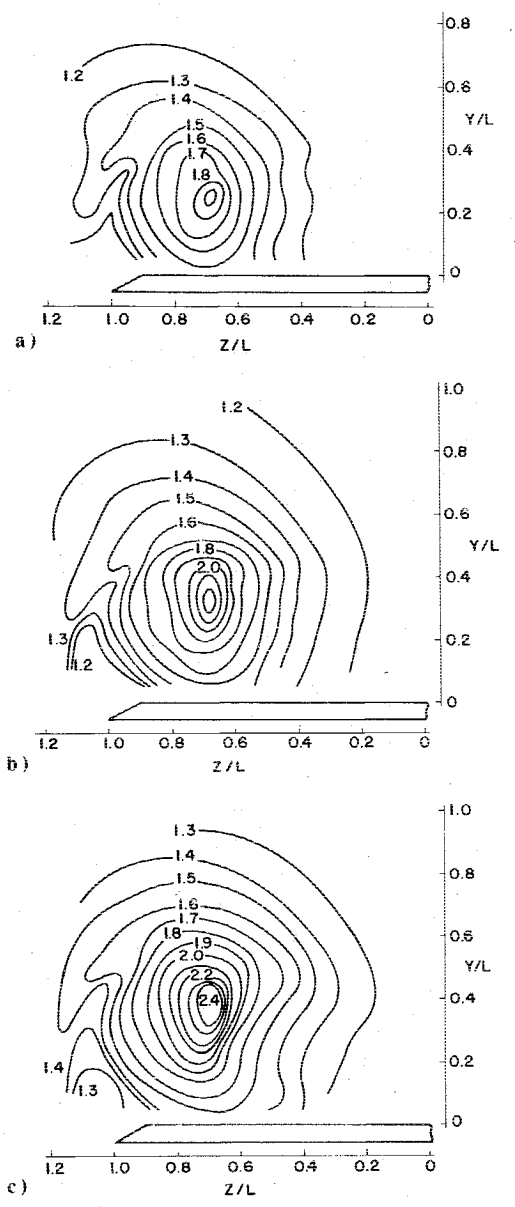

Fig. 4 Contours of constant velocity magnitude over 75-deg sweepback plane delta (Model 1). Numbers denote values of V/V_∞. The angle of attack for this is a) 20 deg, b) 25 deg, c) 29 deg.

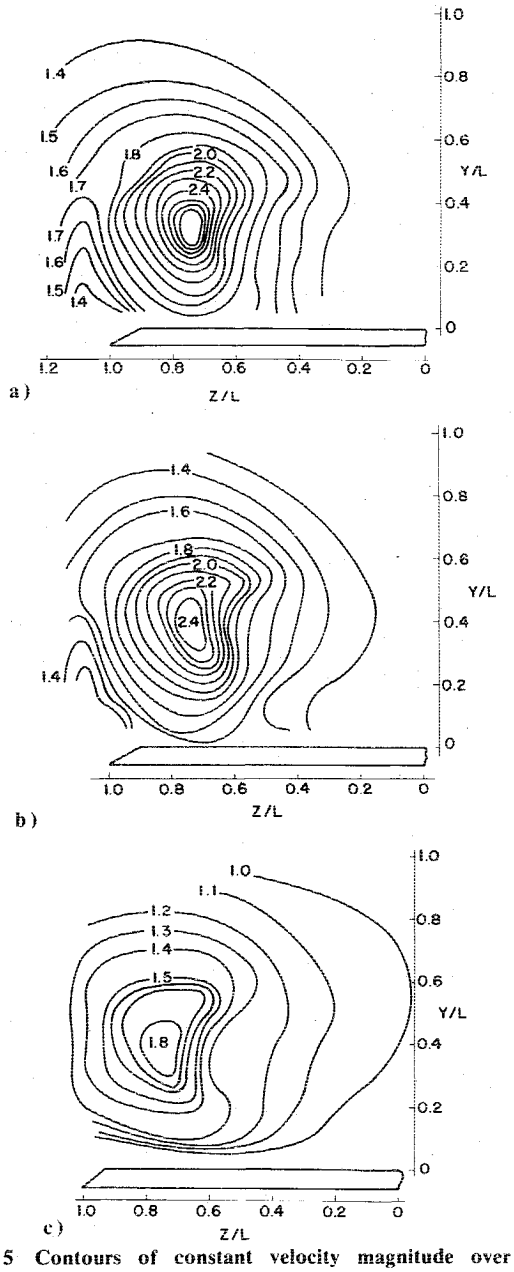

Fig. 5 Contours of constant velocity magnitude over 75-deg sweepback plane delta with flap (Model 2). Numbers denote values of V/V_∞. The angle of attack here is 29 deg and the flap deflection is a) 15 deg down, b) 0 deg, c) 15 deg up.

positions inferred from the contours and some selected profiles of velocity components in the coordinate directions.

Angle of Attack Variation

Effects of angle of attack variation on the vortex flowfield of the basic delta (Model 1) were investigated first. Velocity contours were constructed for 20, 25, and 29 deg angle of attack, as shown in Fig. 4, and serve to illustrate that as α is increased the velocity magnitudes within the vortex increase. It is also shown that the vortex center moves upward with increasing α, which agrees with the generally accepted results for such cases. No apparent movement of the vortex inboard with increasing α was noted in the contours although some slight movement, particularly at low α, has been observed in previous studies.

Camber Variation

In order to determine the effect that the camber of the wing has upon the vortex flowfield, a flap was added to the basic 75-deg delta (Model 2). The angle of attack variation tests were also performed with this model for a flap setting of 15 deg down. The contours from these tests indicate the same general trends mentioned before (increasing vortex strength, vortex center movement upward and very little inboard with increasing angle of attack) and therefore are not shown here. It is worthwhile to mention that the velocity magnitudes are higher (by approximately 12%) and the core heights lower (by approximately 15%) than those for the flat-plate delta at comparable angles of attack. Note here that the angle of attack is measured between the freestream velocity and the centerline chord.

Since the addition of the flap altered the effective area and the aspect ratio compared to the basic delta (Model 1), tests were included where the flap was undeflected. In this manner the effects of the increased area and reduced aspect ratio on the flow could be separated from the effects of the camber variation. The vortex contours for a fixed main panel angle of attack of 29 deg and various flap deflections are shown in Fig. 5. Notice that positive flap deflection strengthens the vortex and brings it closer to the surface, while negative flap deflection weakens the vortex without substantially altering its position.

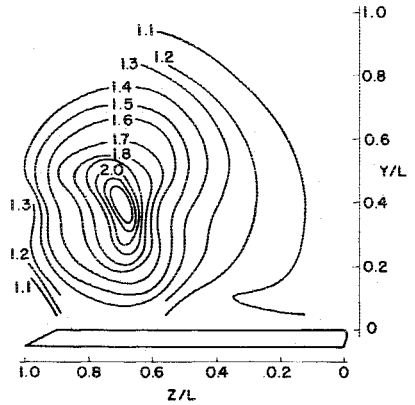

Fig. 6 Contours of constant velocity magnitude over 75-deg sweepback delta with longitudinal curvature (Model 5). Numbers denote values of V/V_∞. The angle of attack is 25 deg.

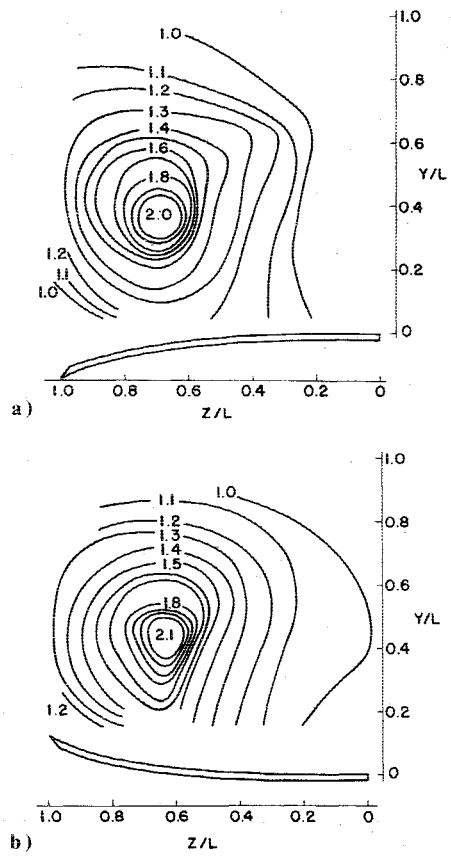

Fig. 7 Contours of constant velocity magnitude over 75-deg sweepback delta with transverse cylindrical curvature (Model 6). Numbers denote values of V/V_∞. The angle of attack is 29 deg, and the curvature is a) concave down b) concave up.

Observation of the enhanced vortex strength possible with flap deflection led to the study of a delta with continuous longitudinal camber. Model 5 was used in this case and velocity magnitude contours for an angle of attack of 25 deg are shown in Fig. 6. Since this is basically a curved version of Model 1, the results obtained can be readily compared to that case. It may be noticed that the major effect of camber is to raise the vortex higher off the surface. That there was no major change in vortex strength is probably because with continuous camber the initial portions of the surface are at relatively small angles to V_∞, while the final portions are at quite larger angles to V_∞. This suggests that over the forward part of the delta the vortex cannot develop appreciable strength, while in the aft region there is difficulty in avoiding

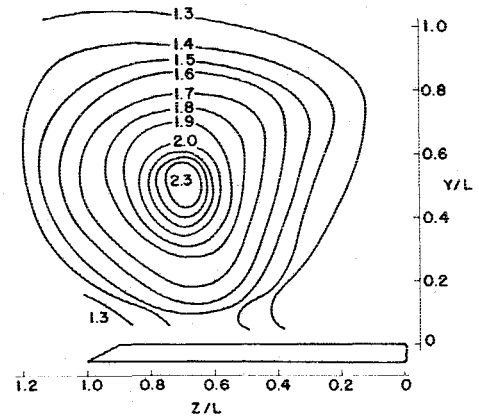

Fig. 8 Contours of constant velocity magnitude over 80-deg sweepback plane delta (Model 3). Numbers denote values of V/V_∞. The angle of attack is 29 deg.

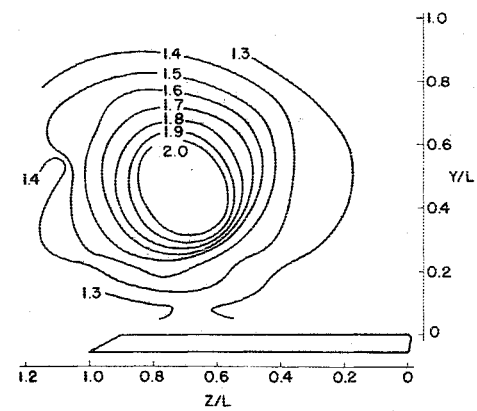

Fig. 9 Contours of constant velocity magnitude over 80-deg sweepback cropped delta (Model 4). Numbers denote values of V/V_∞. The angle of attack is 29 deg.

vortex breakdown. It was observed in our tests that at an angle of attack of 29 deg vortex breakdown would occur over the surface of the model near the measurement station of 0.8 C_0; this made it necessary to test at 25 deg as reported here. Apparently then, continuous longitudinal curvature tends to narrow the operating range of α without any appreciable aerodynamic advantages.

Effects of transverse curvature were briefly examined using Model 6. In this series the cylindrically cambered delta was tested at $\alpha = 29$ deg in two configurations, concave down and concave up; the results of those tests are shown in Fig. 7. The difference in strength of the vortex in each case is slight, the major effect being the alteration of vortex height off the surface. The concave down, or drooped leading-edge case brings the vortex closer to the surface, which enhances its applicability to the design of lifting surfaces. Some studies of the general characteristics of deltas with transverse curvature have been described by Squire.[10]

Sweepback

All cases described thus far have had sweepback angles of 75 deg; it is of interest to indicate the effect of an increase in this angle to 80 deg. Model 3 was constructed for this purpose and it shares with all the other models a span equal to 61 cm. Velocity contours for this model at $\alpha = 29$ deg is shown in Fig. 8. It is seen that the vortex is very high off the surface and the strength is on the order of that found in the 75-deg sweepback case for the same angle of attack. Again the spanwise position is not greatly altered.

The requirement of constant span for all cases studied here is a constraint posed by the use of a delta surface for

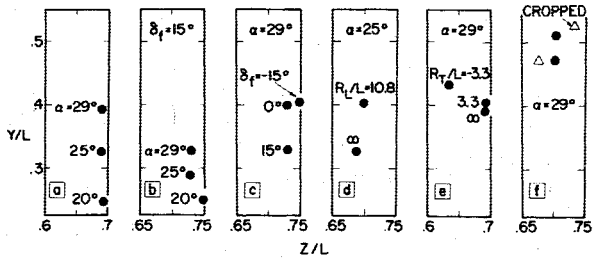

Fig. 10 Location of vortex core inferred from contour plots for the cases: a) Model 1, variation with angle of attack; b) Model 2, flap deflection $\delta_f = 15$ deg, variation with angle of attack; c) Model 2, fixed angle of attack $\alpha = 29$ deg, variation with flap deflection; d) Models 1 and 5, fixed angle of attack $\alpha = 25$ deg, variation of longitudinal curvature; e) Models 1 and 6, fixed $\alpha = 29$ deg, variation of transverse curvature; f) models 3 and 4, fixed sweepback angle of 80 deg, effect of cropping delta.

augmenting natural winds. That is, the half-span essentially sets the size of the rotor which can be used in the vortex above the surface, therefore in assessing the augmenting capability of the various planforms it was decided to fix the half-span for all. The 80-deg sweepback case just described shows the highest vortex position found in this study; this means that the largest rotor for the fixed half-span could be used with this planform. However, this model has the greatest length and area, which is considered, for our purposes, to be a disadvantage. Considering these conditions led to the cropping of this model to form model 4; this model is of the same length as the other models yet it also has 80-deg sweepback. The velocity contours for this cropped delta are shown in Fig. 9. It is seen that the vortex height is only slightly less than that of the complete 80-deg delta and that the strengths are about the same. The central region of the contours, for values of V/V_∞ greater than 2.0, is not shown because in this case the presence of the probe near the center of the core caused the vortex to burst. This was determined by smoke flow visualization of the core while probe was positioned therein. The use of a smaller probe (0.32 cm in diameter) did not cause vortex bursting, but the instrumentation for that probe has not yet been completed, as mentioned in Sec. II.

Vortex Core

The contour data previously described have been used to generate a concise illustration of vortex locations for the cases we have studied and this is shown in Fig. 10. It may be noted that the extent of the excursions of the cores for the various configurations investigated lie in the range $Y/L = 0.35 \pm 50\%$ and $Z/L = 0.70 \pm 10\%$. Thus, it is apparent that the major effect is that due to change in vortex height since there is very little spanwise variation.

The trends noted in this study are in keeping with previous investigations, as typified by the experimental results presented in the review article by Parker.[5] Rather than repeat that information, which is only for flat-plate deltas, it appears sufficient to state that the bounds mentioned earlier for the present data also include the observations of past experiments on core location.

One of the problems associated with leading-edge vortices from low aspect ratio wings at high angles of attack is that of vortex "bursting." This is an abrupt change in the nature of the flow from a well-ordered vortex with a well-defined core to a disordered fluctuating flow with no discernible core; for a discussion of this phenomenon see Hall.[11] Controversy still surrounds the mechanics of the vortex breakdown process, but it is clear that the flow energy available rapidly decreases beyond the burst point. If such an event occurs upstream of a rotor placed in the flow, the energy available to the rotor will be reduced to an extent dependent upon how far upstream of the rotor the burst appears.

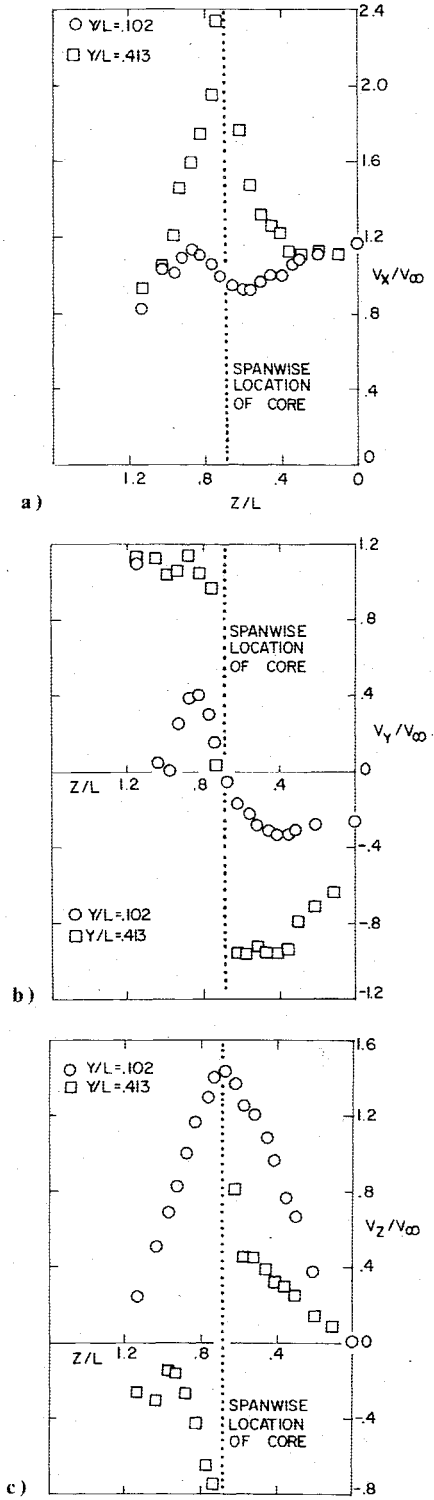

Fig. 11 Spanwise variation of velocity components for Model 1, $\alpha = 29$ deg, at two heights $Y/L = 0.102$ (just above surface) and $Y/L = 0.413$ (slightly above vortex core). Components shown are a) V_x/V_∞, b) V_y/V_∞, c) V_z/V_∞.

The vortex core itself seems to be the sensitive region for the breakdown process. Solid obstructions placed in the core or adverse axial pressure gradients in the outer flow can trigger bursting. Indeed, in wind-tunnel tests with rotor-delta combinations[1,2] it was found that rotor spinner design can influence vortex stability. With the rotor axis aligned with the core axis, bluff spinners sometimes induced breakdown while slender spinners did not do so.

Another factor is the trailing-edge effect, wherein the vortex core faces an adverse axial pressure gradient as

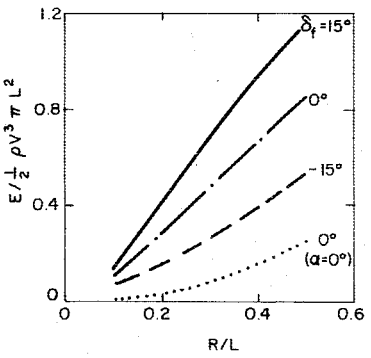

Fig. 12 Energy flow rate through the vortex above Model 2 as a function of nondimensional distance from the center of the vortex for $\alpha = 29$ deg and various flap settings. Energy flow rate is normalized with respect to that in the freestream passing through a streamtube of radius equal to the local half-span L. Lowest curve is for $\alpha = 0$ and $\delta_f = 0$.

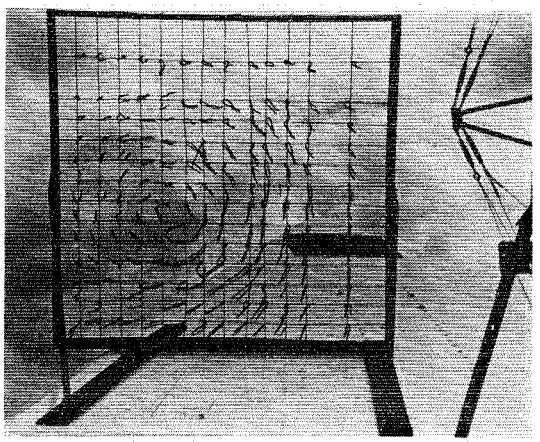

Fig. 13 Photograph of tuft grid visualization of vortex flow over VAC prototype in natural wind at outdoor test site.

relaxation to downstream conditions occurs. This condition prompted the placement of the rotors reasonably far ahead of the trailing edge, e.g., 0.8 C_0. In this fashion the remaining 20% of run of the planform acts to energize the flow downstream of the rotor and thereby decreases the likelihood of vortex breakdown. Of course, the efficacy of this approach, and others under consideration, will be determined by the outcome of further experiments, both in the laboratory and in the field.

Velocity Profiles

It should be apparent from the data thus far presented that the vortex flowfield is quite complicated and that any simplifying assumptions, such as some degree of axisymmetry in the vortex, are to be considered suspect. As mentioned previously, it is difficult to present the data acquired merely because of the great quantity involved. This was the reason for resorting to the use of contours of velocity magnitude. However, in order to give an idea of the variation of the velocity components in the flow, two representative cases are offered. Spanwise variations of V_x/V_∞, V_y/V_∞, and V_z/V_∞ are shown for two different distances from the surface: the lowest traverse taken (3.18 cm off surface) and that passing just above the center of the vortex. The results are for Model 1 at an angle of attack of 29 deg and are shown in Fig. 11.

The spanwise variation of the velocity component in the x direction at the level of the vortex core is seen, in Fig. 11a, to be typical of axial velocity distributions in a vortex. Steep gradients are observed as the core is approached from either side, and a leveling off near the centerline ($Z/L = 0$) is noticed. Near the surface V_x/V_∞ exhibits some fluctuations about a value of 1.0. It is probable that boundary-layer studies of such flows will have difficulties considering this effect.

The component V_y/V_∞ again illustrates the strong vortex nature of the flow at the core height with downflow at the inboard stations and upflow at the outboard stations as seen in Fig. 11b. Near the surface it is interesting to note that the downflow over the inboard section goes to zero at the spanwise location of the core. Then the flow is directed upward until it weakens toward zero at the leading edge.

Finally, the V_z/V_∞ component is seen also to illustrate the vortex character at the level of the vortex core as shown in Fig. 11c. Near the surface the spanwise scrubbing action of the vortex is vividly illustrated; notice the peak in V_z/V_∞ lies directly under the vortex core.

IV. Applications to Wind Energy Conversion

Power Control

Experimental results for the vortex velocity components taken from the previously mentioned studies indicate that, not only are the axial velocity components in the vortex appreciably larger than the freestream velocity, but, in addition, there is a circumferential velocity component present whose magnitude is on the order of that of the freestream velocity. It is clear that the energy flux in the vortex is considerably greater than that of the undisturbed oncoming flow. This then is the augmenting effect of the vortex generating surface: it amplifies the wind speed within the vortex field in that the swirling flow tends to concentrate the low energy flux wind from a large upstream area into a high energy flux flow in a small (vortex) area.

Flowfield energy flux distributions as a function of radius from the vortex center may be calculated from the detailed velocity distributions. For the flat-plate delta mentioned previously, the power distribution in the flow above one-half (the port half) of the surface at $x = 0.8$ C_0, nondimensionalized with respect to the power in the undisturbed stream over a streamtube whose radius is equal to the local semispan $L(x)$ is shown in Fig. 12 for various conditions. The available power increases with increasing angle of attack for the basic flat-plate case, but these results are not shown. However, at a given angle of attack $\alpha = 29$ deg the available power increases when a flap is deflected 15 deg down and decreases when the flap is deflected up 15 deg. Note that the case $\alpha = 0$ corresponds to no vortex augmentation; the rotor in this case would face an essentially undisturbed wind stream.

It is clear then that there is an additional degree of freedom in vortex augmentor wind energy systems: the power available to the rotor may be altered by merely changing the angle of attack or by deflecting a flap. Thus, operation at high angles of attack can provide power under quite low wind conditions while under high wind conditions the power load may be reduced by reducing the angle of attack of the augmentor surface or by deflecting a flap rather than by rotor blade pitch changes.

Rotor Considerations

Turbines for transforming the flow power to shaft power are subject to the whirling vortex flow described previously. As the velocity contour plots show, the vortex augmentor surface acts so as to process the wind prior to its reaching the turbine. That is, the translating movement of the wind is transformed into a rotating and translating movement by the augmentor surface. Nonuniformities in the wind profile will tend to be smoothed out during the process of vortex formation and propagation.

This preprocessing also gives a predictable, ordered direction of rotation for the vortices. This is analogous to prewhirl or prerotation in turbomachinery where it is often used to great advantage. Because of this prerotation effect,

much higher effective tip speeds are possible with vortex augmentor systems. When the small size of the rotors required by the VAC system is also considered it is evident that very high rotational speeds are possible. In this fashion there are reduced requirements for step-up transmissions to the generator or else a higher-speed generator may be used. Generators with high operating speeds are generally lighter and less expensive than their lower-speed counterparts for the same power rating. In addition, the reduced inertia of the light, high-speed rotor-transmission-generator system possible with VAC systems should provide better response to temporal wind speed variations.

VAC Prototype

Having carried out a great deal of basic research and experimentation on laboratory scale systems which validated the vortex augmentor concept, consideration was given to development of a prototype for field testing. A simple flat-plate delta planform with 75-deg sweepback was chosen for the prototype augmentor surface. The vortex field above the augmentor surface of the prototype was made visible by means of a large (1.2×1.2 m) tuft grid mounted on the port side as shown in Fig. 13, where a well-developed vortex is clearly evident. The complete prototype has been instrumented and is presented under field test at our test site, which includes a complete wind sensor network tied in to an on-line minicomputer. The details of the prototype and field test program are reported in Ref. 12.

Acknowledgment

This work was supported in part by U. S. Energy Research and Development Administration, under Contract No. E(49-18)-2358, and the National Science Foundation, under Grant No. AER 7500850. The authors wish to thank Martin H. Bloom for his helpful suggestions and encouragement.

References

[1] Sforza, P. M., "Vortex Augmentor Concepts for Wind Energy Conversion," *Proceedings of the Second Workshop on Wind Energy Conversion Systems*, Washington, D.C. June 9-11, 1975; the MITRE Corp., Sept. 1975.

[2] Sforza, P. M., "Vortex Augmentors for Wind Energy Conversion," *International Symposium on Wind Energy Systems*, Cambridge University, England, Sept. 7-9, 1976; British Hydromechanics Research Association.

[3] Sforza, P. M., "Aircraft Vortices—Benign or Baleful," *Space/Aeronautics*, April 1970, pp. 42-48.

[4] Thwaites, B., *Incompressible Aerodynamics*, Oxford University Press, London, 1960.

[5] Parker, A. G., "Aerodynamic Characteristics of Slender Wings with Sharp Leading Edges—A Review," *Journal of Aircraft*, Vol. 13, March 1976, pp. 161-168.

[6] Timm, G. K., "Survey of Experimental Velocity Distributions in Vortex Flows, with Bibliography," Boeing Scientific Research Laboratories, Document DI-82-0683, Nov. 1967.

[7] Earnshaw, P. B., "An Experimental Investigation of the Structure of a Leading Edge Vortex," ARC R&M No. 3281, March 1961.

[8] Hall, M. G., "A Theory for the Core of a Leading Edge Vortex," *Journal of Fluid Mechanics*, Vol. 11, 1966, p. 209.

[9] Hummel, D., "Untersuchungen uber das Aufplatzen der Wirbel an Schlanken Deltaflugeln," *Zeitschrift fur Flugwissenshaft*, Vol. 13, Heft 5, 1965.

[10] Squire, L. C., "Camber Effects on the Nonlinear Lift of Slender Wings with Sharp Leading Edges," ARC C.P. No. 924, 1967.

[11] Hall, M. G., "The Structure of Concentrated Vortex Cores," *Progress in Aeronautical Science*, Vol. 7, Pergamon Press, New York, 1966, pp. 53-110.

[12] Sforza, P. M., "Vortex Augmentation of Wind Energy," *Wind Engineering*, Vol. 1, No. 3 (to appear).